Acidosis-Sensing Glutamine Pump SNAT2 Determines Amino Acid Levels and Mammalian Target of Rapamycin Signalling to Protein Synthesis in L6 Muscle Cells

Kate Evans,* Zeerak Nasim,* Jeremy Brown,* Heather Butler,* Samira Kauser,* Hélène Varoqui,† Jeffrey D. Erickson,† Terence P. Herbert,‡ and Alan Bevington*

**Department of Infection, Immunity and Inflammation, University of Leicester, John Walls Renal Unit, Leicester General Hospital, and ‡Department of Cell Physiology and Pharmacology, University of Leicester, Leicester, United Kingdom; and †Neuroscience Center, Louisiana State University Health Sciences Center, New Orleans, Louisiana*

Wasting of lean tissue as a consequence of metabolic acidosis is a serious problem in patients with chronic renal failure. A possible contributor is inhibition by low pH of the System A (SNAT2) transporter, which carries the amino acid L-glutamine (L-Gln) into muscle cells. The aim of this study was to determine the effect of selective SNAT2 inhibition on intracellular amino acid profiles and amino acid–dependent signaling through mammalian target of rapamycin in L6 skeletal muscle cells. Inhibition of SNAT2 with the selective competitive substrate methylaminoisobutyrate, metabolic acidosis (pH 7.1), or silencing SNAT2 expression with small interfering RNA all depleted intracellular L-Gln. SNAT2 inhibition also indirectly depleted other amino acids whose intracellular concentrations are maintained by the L-Gln gradient across the plasma membrane, notably the anabolic amino acid L-leucine. Consequently, SNAT2 inhibition strongly impaired signaling through mammalian target of rapamycin to ribosomal protein S6 kinase, ribosomal protein S6, and 4E-BP1, leading to impairment of protein synthesis comparable with that induced by rapamycin. It is concluded that even though SNAT2 is only one of several L-Gln transporters in muscle, it may determine intracellular anabolic amino acid levels, regulating the amino acid signaling that affects protein mass, nucleotide/nucleic acid metabolism, and cell growth.

J Am Soc Nephrol 18: 1426–1436, 2007. doi: 10.1681/ASN.2006091014

Cachexia, the wasting of soft tissue, particularly skeletal muscle, is a frequent occurrence in patients with ESRD and is particularly severe in patients with diabetic nephropathy (1). It is a serious clinical problem because of its strong association with morbidity and mortality. An important cause is uremic metabolic acidosis (2), and there is good evidence that correction of acidosis decreases both weight loss and morbidity (3,4). Depletion of intramuscular free amino acids is thought to be an important early step in muscle wasting in uremia (5), and depletion is reversed if acidosis is corrected (6). Intracellular amino acid depletion is sensed through mammalian target of rapamycin (mTOR), a well-documented mechanism through which amino acids stimulate protein synthesis (7). Impaired protein synthesis is an early consequence of metabolic acidosis in humans (8) and is partly compensated for by harvesting of amino acids at the expense of protein degradation (9,10), but precisely how acidosis leads to the initial amino acid depletion is poorly understood.

Availability of the free amino acid L-glutamine (L-Gln) limits protein synthesis (11), protein degradation (12), and nucleotide and nucleic acid biosynthesis (13) in some cell types. Consequently, L-Gln has been proposed as a key factor in growth and maintenance of mammalian tissues (14), and L-Gln availability and losses from muscle may be important contributors to wasting illness and clinical outcome in seriously ill patients (15). A crucial factor is active transport of L-Gln across the plasma membrane (15), maintaining an intracellular concentration at least 20 times higher than the 0.5 to 1 mM found in extracellular fluid (16). In muscle the molecular identity of the transporter(s) involved has been obscure, but studies in cultured L6 skeletal muscle cells (17,18) have implicated System A neutral amino acid transporters of the SNAT/slc38 transporter family, in particular SNAT2 (19). SNAT2 is also a possible mediator of the effects of acidosis because it is strongly inhibited at low pH (20).

This study investigated the SNAT2 transporter in L6 muscle cells as a potential target through which catabolic stimuli trigger protein wasting. We demonstrate, for the first time, that inhibition of SNAT2 alone is sufficient to deplete intracellular L-Gln and other anabolic amino acids, that metabolic acidosis gives similar depletion, and that SNAT2 is consequently a potential regulator of amino acid–dependent signaling to mTOR and hence to protein synthesis.

Received September 15, 2006. Accepted February 19, 2007.

Published online ahead of print. Publication date available at www.jasn.org.

Address correspondence to: Dr. Alan Bevington, Department of Infection, Immunity and Inflammation, University of Leicester, John Walls Renal Unit, Leicester General Hospital, Leicester LE5 4PW, UK. Phone: +44-116-258-8041; Fax: +44-116-273-4989; E-mail: ab74@leicester.ac.uk

Materials and Methods

Cell Culture

L6-G8C5 rat myoblasts were grown to confluence in DMEM with 10% vol/vol FBS and fused to form myotubes by culturing in Minimum

ISSN: 1046-6673/1805-1426

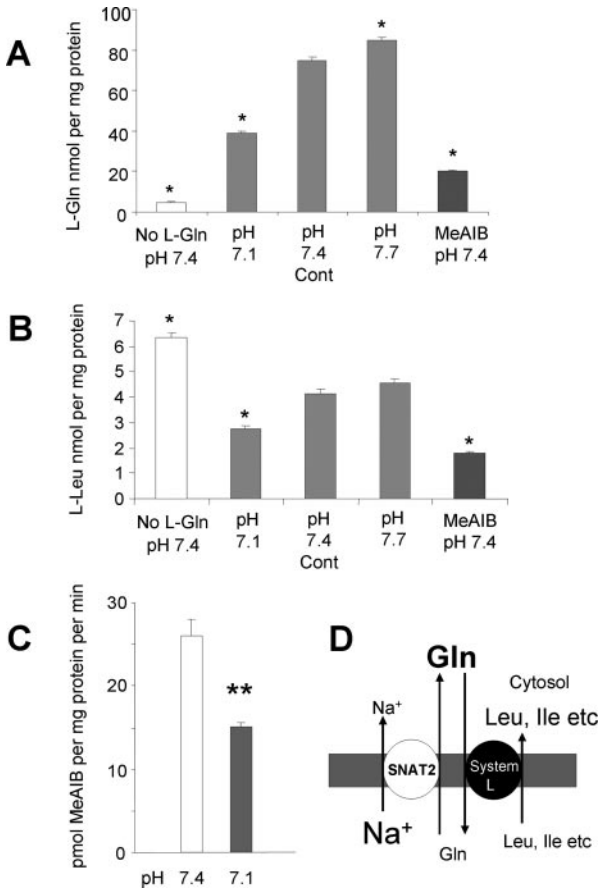

Figure 1. Effect of 2 h of extracellular L-glutamine (L-Gln) starvation, pH variation, or inhibition of SNAT2 transporters with 10 mM methylaminoisobutyrate (MeAIB) on intracellular concentrations of L-Gln (A) and L-leucine (L-Leu; B) in L6-G8C5 myotubes. (Data for other amino acids are presented in Table 1.) All media contained 2 mM L-Gln and 0.4 mM L-Leu unless otherwise stated. *$P < 0.05$ *versus* control medium (Cont). Results from one experiment representative of four independent experiments are shown ($n = 5$ replicate culture wells for each treatment). (C) Effect of extracellular pH on SNAT2 transporter activity after 7 h of exposure to experimental media at the specified pH. Transport was then immediately assessed from the rate of uptake of ^{14}C-MeAIB in HEPES-buffered saline at the same pH as the experimental media (18). Results from one experiment representative of three independent experiments are shown ($n = 3$ replicate culture wells for each treatment). **$P < 0.05$ *versus* the corresponding medium at pH 7.4. (D) Schematic diagram of coupling between SNAT2 and System L amino acid transporters. Larger lettering for a given solute denotes higher concentration. L-Gln influx into the cytosol through SNAT2 (coupled to the electrochemical gradient of Na^+ across the plasma membrane) drives accumulation of a high concentration of L-Gln and other SNAT2 substrates in the cytosol. Subsequent efflux of this accumulated L-Gln on plasma membrane amino acid exchangers such as System L then drives secondary accumulation in the cell of other amino acids, such as L-Leu, which are poor substrates for SNAT2.

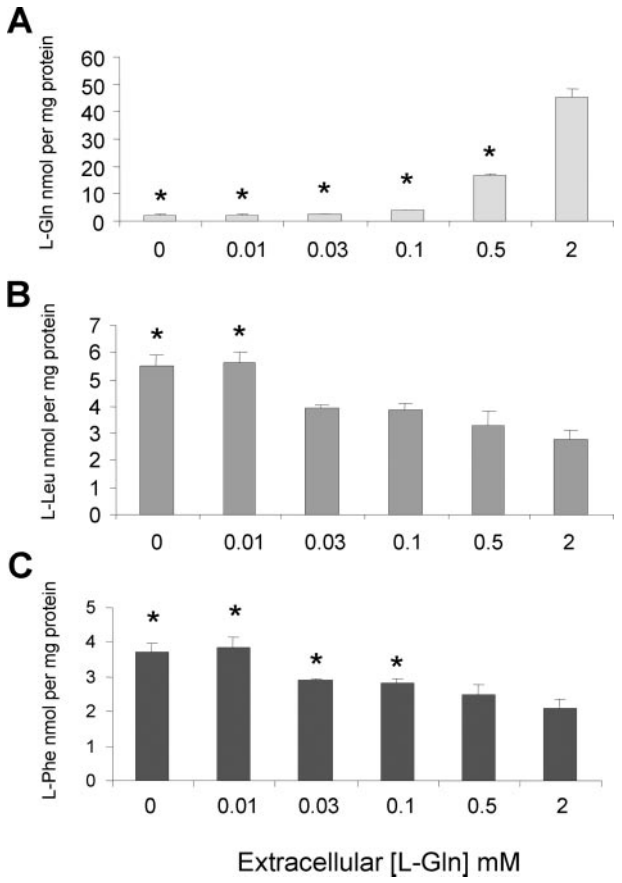

Figure 2. Effect of extracellular L-Gln concentration on intracellular concentrations of L-Gln (A), L-Leu (B), and L-phenylalanine (L-Phe; C) after 2 h at pH 7.4. *$P < 0.05$ *versus* medium with 2 mM L-Gln. Results from one experiment representative of three independent experiments are shown ($n = 3$ replicate culture wells for each treatment).

Essential Medium with 2% (vol/vol) FBS as described previously (18). For experiments with unfused myoblasts, cells were seeded in DMEM/10% serum at $3.4 \times 10^4/cm^2$, fresh medium was added after 24 h, and myoblasts were used after an additional 17 h. Unless otherwise stated, experimental incubations were performed in Minimum Essential Medium with 2 mM L-Gln, penicillin (10^5 IU/L), streptomycin (100 mg/L), and 2% (vol/vol) dialyzed FBS. At the end of experimental incubations, lysates for mTOR signaling studies and a 170,000 × *g* total membrane fraction that contained SNAT2 were prepared as described previously (21,22).

Protein synthesis rate was determined from incorporation of L-[2,6 ^{3}H]-phenylalanine ([2,6 ^{3}H]-Phe; Amersham TRK552, Little Chalfont, UK) into protein (22) during a 4-h incubation at the end of the experiment, in the specified experimental medium. The concentration of ^{3}H-L-Phe in the medium was 2 mCi (74 MBq)/L, and total L-Phe concentration was 600 μmol/L. For the acute 2-h experiment, the incubation was with 2 mCi (74 MBq)/L ^{3}H-L-Phe and 200 μmol/L L-Phe for 30 min. Cultures were then rinsed three times on ice with 0.9% (wt/vol) NaCl and scraped in 10% (wt/vol) TCA to precipitate labeled protein. Total protein and DNA were determined as described previously (18), and protein synthesis is expressed as nanomoles of L-Phe incorporated per milligram of protein.

Protein degradation was measured by prelabeling cell protein with ^{3}H-L-Phe and measuring release of acid-soluble radioactivity into the medium (23), expressed as $\log_{10}$ of the percentage of the total initial cellular ^{3}H per hour (23). Cell viability was assessed from release of acid-precipitable radioactivity into the medium, an indicator of intact

Table 1. Effect of extracellular L-Gln starvation, pH, and SNAT2 inhibition with MeAIB on intracellular free amino acid profile in L6-G8C5 myotubes after 2-h incubations[a]

Parameter		Composition of the Medium				
pH		7.4	7.1	7.4 (Control)	7.7	7.4
L-Gln (mmol/L)		0	2	2	2	2
MeAIB (mmol/L)		0	0	0	0	10
Amino acid	Concentration in fresh MEM (μmol/L)	Intracellular Free Amino Acid Concentration (nmol/mg protein)				
L-Ala	Nil	75.9 ± 2.1	71.3 ± 1.3	70.0 ± 1.7	69.3 ± 2.5	69.4 ± 1.6
L-Arg	600	5.23 ± 0.15[c]	3.99 ± 0.08[c]	4.68 ± 0.12	4.94 ± 0.11	3.38 ± 0.11[c]
L-Asn	Nil	0.54 ± 0.05[c]	1.28 ± 0.05[c]	1.43 ± 0.05	1.34 ± 0.03	0.92 ± 0.02[c]
L-Asp	Nil	25.6 ± 1.3[c]	37.4 ± 1.2[c]	47.4 ± 1.5	47.0 ± 0.6	43.8 ± 0.7
L-Cys	200[b]	UD	UD	UD	UD	UD
L-Glu	Nil	28.3 ± 1.3[c]	37.0 ± 0.8[d]	42.2 ± 2.1	48.8 ± 3.0[c]	38.8 ± 2.0
Gly	Nil	13.1 ± 0.5	14.4 ± 0.5[c]	12.1 ± 0.2	10.4 ± 0.2[c]	12.9 ± 0.3
L-His	200	3.6 ± 0.2[c]	1.2 ± 0.1[c]	2.4 ± 0.3	2.7 ± 0.2	0.8 ± 0.1[c]
L-Ile	400	5.5 ± 0.2[c]	2.5 ± 0.1[c]	3.7 ± 0.2	3.9 ± 0.2	1.7 ± 0.1[c]
L-Lys	400	UD	UD	UD	UD	UD
L-Met	100	3.7 ± 0.3[c]	1.2 ± 0.2[d]	1.8 ± 0.3	2.3 ± 0.3	1.1 ± 0.2
L-Phe	200	4.39 ± 0.12[c]	1.92 ± 0.08[c]	2.82 ± 0.09	3.14 ± 0.07	1.29 ± 0.04[c]
L-Pro	Nil	1.5 ± 0.1[c]	3.9 ± 0.3	3.4 ± 0.2	3.4 ± 0.2	2.4 ± 0.1[c]
L-Ser	Nil	1.81 ± 0.06	1.53 ± 0.06	1.60 ± 0.05	1.58 ± 0.06	1.29 ± 0.05[c]
L-Thr	400	36.1 ± 1.1[c]	15.3 ± 0.5[c]	20.2 ± 0.4	25.9 ± 0.4[c]	9.4 ± 0.2[c]
L-Trp	50	1.40 ± 0.05[c]	0.69 ± 0.05[c]	0.98 ± 0.05	1.01 ± 0.04	0.52 ± 0.02[c]
L-Tyr	200	4.79 ± 0.15[c]	2.32 ± 0.38[c]	3.12 ± 0.15	3.41 ± 0.14	1.42 ± 0.06[c]
L-Val	400	6.03 ± 0.19[c]	3.06 ± 0.14[c]	4.05 ± 0.19	4.32 ± 0.19	2.59 ± 0.08[c]

[a]Data for L-Gln and L-Leu are presented in Figure 1. Results from one experiment representative of four independent experiments are shown ($n = 5$ replicate culture wells for each treatment). Ala, alanine; Arg, arginine; Asn, asparagine; Asp, aspartic acid; Cys, cysteine; Glu, glutamic acid; Gly, glycine; His, histidine; Ile, isoleucine; Lys, lysine; MeAIB, methylaminoisobutyrate; MEM, Minimum Essential Medium; Met, methionine; Phe, phenylalanine; Pro, proline; Ser, serine; Thr, threonine; Trp, tryptophan; Tyr, tyrosine; Val, valine; UD, undetectable.
[b]Added as cystine.
[c]$P < 0.05$ *versus* pH 7.4 control.
[d]$P < 0.05$ *versus* pH 7.7.

protein leakage and cell detachment (24). Release is expressed as percentage of the total initial cellular ^3H per hour.

SNAT2 transporter activity was assayed from uptake of ^{14}C-methylaminoisobutyrate (MeAIB; NEN-Du Pont, Beaconsfield, UK) into intact myotubes during 5-min incubations (25) with 10 μmol/L MeAIB at 0.5 mCi (18.5 MBq)/L. For subconfluent myoblasts, this was increased to 40 μmol/L at 2 mCi (74 MBq)/L.

Amino Acid Analysis

Cultures on 35-mm wells were rapidly chilled on ice, rinsed three times with ice-cold 0.9% (wt/vol) NaCl, and deproteinized by scraping in 150 μl of 0.3 M perchloric acid. Precipitated protein was sedimented (10 min, 4°C, 3000 × *g*) and retained for total protein assay. Supernatant was neutralized by vortexing with an equal volume of tri-n-octylamine/1,1,2-trichloro, trifluoro-ethane (22:78 vol/vol) (26). The top (neutralized aqueous) phase was stored at −80°C. Amino acids were determined on an Agilent 1100 high-performance liquid chromatograph with Zorbax Eclipse AAA column (4.6 × 75 mm, 3.5 μm) at 40°C with *o*-phthalaldehyde/3-mercaptopropionate/9-fluorenylmethylchloroformate precolumn derivatization and ultraviolet and fluorimetric postcolumn detection.

SDS-PAGE and Immunoblotting

Cell lysates or membranes (20 μg protein per lane) were subjected to SDS-PAGE, and proteins were blotted onto nitrocellulose membranes (Amersham Hybond ECL). Membranes were blocked for 1 h at room temperature with Tris-buffered saline (pH 7.6) with 5% (wt/vol) skim milk and 0.1% (vol/vol) Tween 20 detergent, and then probed with primary antibodies in blocking buffer at 4°C overnight. Anti-SNAT2 rabbit polyclonal antibody (raised against the N-terminal hydrophilic portion of rat SNAT2 [amino acids 1 to 65] and characterized previously [27]) was used at 1:4000 dilution. Anti–α_1-Na,K-ATPase mouse monoclonal (Abcam, Cambridge, UK) was used at 1:5000. Antibodies against ribosomal protein (rp) S6-kinase (New England Biolabs, Hitchin, UK) and phosphorylated rpS6 and 4E-BP1 were used at 1:1000 dilution. Primary antibody was detected using horseradish peroxidase–conjugated goat anti-rabbit IgG or rabbit anti-mouse IgG (Dako, Ely, UK) at 1:1500 dilution for 2 h in blocking buffer at room temperature. Horseradish peroxidase–labeled bands were detected by chemiluminescence (ECL; Amersham) and quantified with a Bio-Rad GS700 densitometer (Bio-Rad, Hemel Hempstead, UK) using Molecular Analyst v1.4 software.

RNA Isolation and Reverse Transcriptase–PCR

RNA was isolated from cells using TRIzol (Invitrogen) and quantified by spectrophotometry at 260 nm. RNA was reverse-transcribed using an AMV Reverse Transcription System (Promega A3500, Madison, WI) and was amplified by PCR using the following gene-specific primers: Rat SNAT1 (28) (493-bp product), forward 5′-CTGATCGGGAGAGTAGGAGGAGTC-3′ and reverse 5′-AGCGGGAGAATTAT-

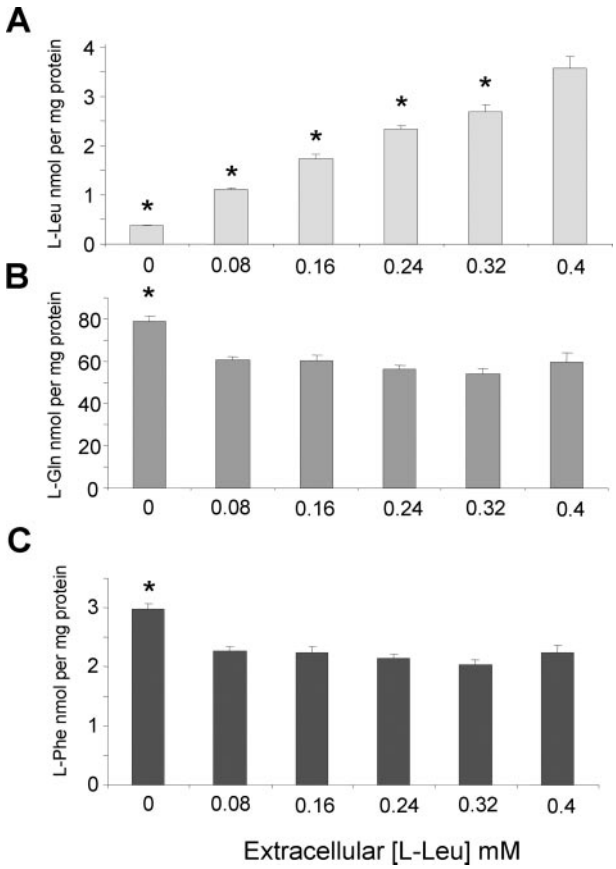

Figure 3. Effect of extracellular L-Leu concentration on intracellular concentrations of L-Leu (A), L-Gln (B), and L-Phe (C) after 2 h at pH 7.4. *$P < 0.05$ *versus* medium with 0.4 mmol/L L-Leu. Pooled results from three independent experiments are shown with duplicate culture wells for each treatment in each experiment.

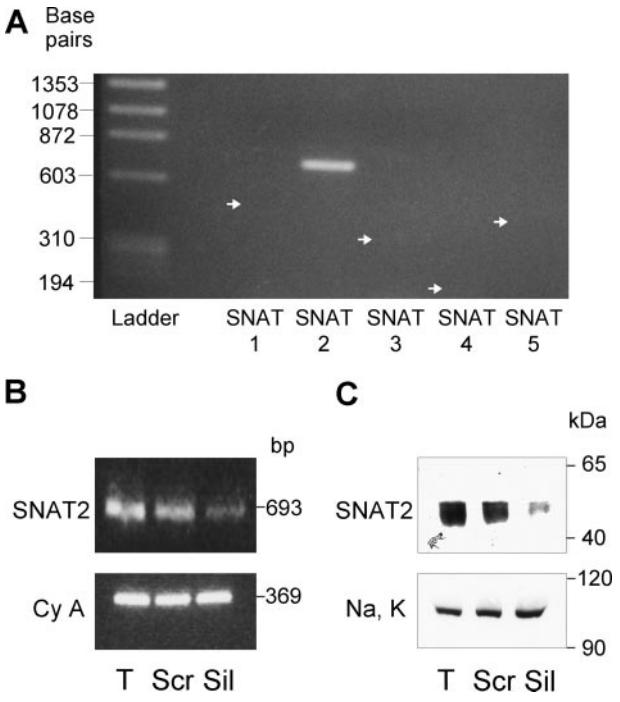

Figure 4. (A) Detection of SNAT (slc38 gene family) expression in L6-G8C5 myoblasts by reverse transcriptase–PCR (RT-PCR) using specific oligonucleotide primers (see Materials and Methods). Only SNAT2 expression was detected. White arrows denote the size of the PCR products expected with the primers for SNAT1 and SNAT3 to 5. "Ladder" is a PhiX174 HaeIII DNA digest (Sigma D-0672). (B) Confirmation of small interfering RNA (siRNA) silencing of SNAT2 expression in L6-G8C5 myoblasts by RT-PCR using the same SNAT2-specific PCR primers as in A and Cyclophilin A primers "CyA" as a loading control. T, transfection blank (cells that were exposed to calcium phosphate transfection agent only); Scr, cells that were exposed to scrambled control siRNA; Sil, cells that were exposed to SNAT2-silencing siRNA. (C) Confirmation of siRNA silencing of SNAT2 expression by immunoblotting of proteins that were separated by SDS-PAGE from a 170,000 × *g* membrane fraction that was derived from L6-G8C5 myoblasts that were incubated with siRNA or transfection agent as in B. Proteins were probed with SNAT2-specific antibody or α_1-Na, K-ATPase antibody "Na,K" as a loading control. Results are representative of three independent experiments.

GCCAAAGGTT-3′; rat SNAT2 (28) (693-bp product), forward 5′-TACGAACAGTTGGGACATAAGG-3′ and reverse 5′-AGTTCCCACGATCGCAGAGTAG-3′; rat SNAT3 (29) (337-bp product), forward 5′-TTGGGCATATTTGGGATCATTGGTG-3′ and reverse 5′-TCCCCTGTCTTTCTCCCCTTCCTTA-3′; rat SNAT4 (30) (187- product), forward 5′-ACCCTGGAACGACCTCTTTT-3′ and reverse 5′-CCTTCCTTGGCTGTCTTCAG-3′; rat SNAT5 (29) (424-bp product), forward 5′-TCAGCCCCTAGCCTCATCTTCATCC-3′ and reverse 5′-AGCTGGCCTCCCTTCCTCCTCTC-3′; and rat Cyclophilin A (31) (369-bp product), forward 5′-CAACCCCACCGTGTTCTTCG-3′ and reverse 5′-TTGCCATCCAGCCACTCAGTC-3′. Amplification was performed using Abgene Reddymix System (Abgene AB-0575/LD/b, Rochester, NY), with the following PCR amplification conditions: 94°C for 4 min, then 25 cycles that comprised 94°C for 30 s, 55°C for 1 min, and 68°C for 1 min, followed by a final single extension step of 68°C for 7 min. Reverse transcriptase–PCR products were resolved on 1.5% (wt/vol) agarose in 40 mM Tris-acetate and 1 mM EDTA (pH 8.3) with 0.5 μg/ml ethidium bromide and visualized by ultraviolet fluorescence.

Small Interfering RNA Transfection

Because confluent cultures (including myotubes) show limited transfection with small interfering RNA (siRNA) oligonucleotides, myoblasts (40% confluent) were used for siRNA transfection. Their ability to take up siRNA was confirmed with fluorescein-labeled double-stranded random siRNA (Qiagen 1022081, Crawley, UK) followed by quantification by flow cytometry. For SNAT2 silencing, myoblasts were transfected with the following double-stranded siRNA at a final concentration of 30 nM for 16 h in DMEM/10% FBS using Profection Calcium Phosphate transfection (Promega E1200): (*1*) SNAT2 silencing siRNA (forward sequence 5′-CUGACAUUCUCCUCCUCGUdTdT directed against base position 1095 onward in the gene sequence) and (*2*) scrambled control siRNA (forward sequence 5′-CGCUCUACUCUACUUGUCCdTdT) sharing the same base composition as (*1*) but in random sequence. After transfection, cultures were incubated in fresh DMEM/10% FBS for 24 h before commencing measurements.

Statistical Analyses

Data are presented as means ± SE. Statistical significance was assessed by ANOVA and *post hoc* testing with Duncan multiple range

test, using SPSS 11.01 (SPSS, Chicago, IL). Changes were regarded as significant at $P < 0.05$.

Results

SNAT2 Inhibition Depletes Intracellular Amino Acids

For investigation of whether SNAT2 has a role in maintaining intracellular L-Gln concentration, this transporter was subjected to selective competitive inhibition by incubation of L6 myotubes with a saturating dose of the specific substrate MeAIB. Intracellular L-Gln was strongly depleted (by 75%) after only 2 h (Figure 1A). Partial (approximately 40%) inhibition of SNAT2 transporter activity was also achieved by acidosis (*i.e.*, by lowering the pH of the medium to 7.1 [Figure 1C]). As expected, this inhibitory effect on SNAT2 led to a commensurate depletion of L-Gln (Figure 1A).

SNAT2 inhibition also led to significant depletion of L-leucine (L-Leu; Figure 1B), another amino acid that exerts a protein anabolic effect in human muscle (32) and L6 cells (33,34). L-Leu is not a substrate for SNAT2 (27), and MeAIB is not a substrate for the System L transporters of the slc7 family that carry L-Leu (35). This suggests that coupling occurs between SNAT2 and System L transporters, possibly mediated by the transmembrane L-Gln gradient and 1:1 exchange of L-Gln for L-Leu (see Figure 1D and the Discussion section). To demonstrate that the L-Gln gradient is involved in active accumulation of L-Leu inside the cells, L-Gln was removed from the extracellular medium. This depleted intracellular L-Gln, but after 2 h, the concentration inside the cells was still appreciable: Approximately 4 nmol/mg protein (Figure 1A). The inside/outside concentration gradient (4 divided by 0, *i.e.*, tending to infinity) was therefore considerably larger than in the control cultures and led to the predicted enhanced accumulation of L-Leu in the cells (Figure 1B). This effect of extracellular L-Gln depletion on intracellular L-Leu was dosage-dependent (Figure 2, A and B) and also led to the expected intracellular accumulation of other System L substrates with bulky side chains such as L-Phe (Figure 2C) and L-isoleucine (L-Ile), L-valine (L-Val), L-tyrosine (L-Tyr), and L-tryptophan (L-Trp; Table 1). For providing further evidence that inside/outside transmembrane gradients of System L amino acids can drive intracellular accumulation of other System L substrates, a steep transmembrane inside/outside gradient of L-Leu was imposed by removal of extracellular L-Leu (Figure 3A). Despite the much smaller mass of L-Leu than L-Gln in both intracellular and extracellular fluid, this led as predicted to a small but reproducible increase in intracellular L-Gln (Figure 3B) and L-Phe (Figure 3C).

Silencing of SNAT2 Gene Expression

To confirm that the predominant System A transporter gene that is expressed in L6-G8C5 cells is SNAT2, we examined expression of all five slc38 family transporters using gene-specific PCR primers. In agreement with earlier studies in L6 myotubes (28) and in rat skeletal muscle *in vivo* (27), only SNAT2 was detected (Figure 4A). The dominant role of SNAT2 in L-Gln and L-Leu homeostasis was confirmed in L6-G8C5 myoblasts by silencing SNAT2 expression using siRNA. SNAT2 silencing was demonstrated by reverse transcriptase–PCR (Figure 4B) and Western blotting (Figure 4C) and by functional assay of transporter activity (Figure 5A). Whereas the silencing siRNA significantly reduced SNAT2 expression (Figure 4, B and C), transfection agent or scrambled control siRNA had no effect.

In Figure 5A, the severity of SNAT2 transporter inhibition with the silencing siRNA was comparable with that observed during acidosis (Figure 1C). As expected, depletion of L-Gln, of branched-chain amino acids (L-Leu, L-Ile, and L-Val), of aromatic amino acids (L-Phe, L-Tyr, and L-Trp), and of L-histidine, L-methionine, and L-threonine (Figure 5, Table 2) was similar to that observed in myotubes at pH 7.1 (Figure 1, Table 1). In contrast, scrambled siRNA, when compared with transfection agent alone, had a negligible effect, exerting a statistically significant effect only on glycine (Table 2).

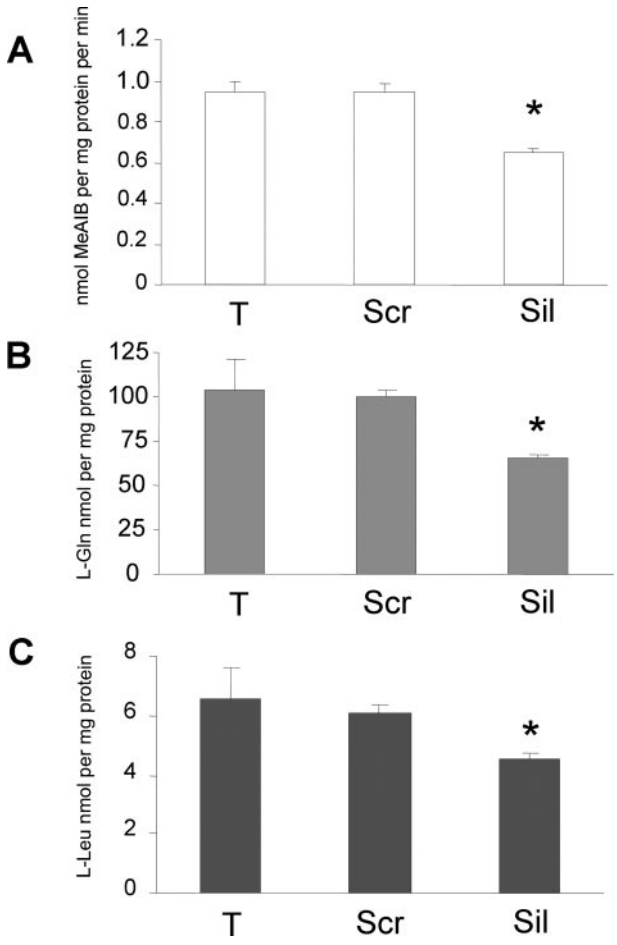

Figure 5. Effect of SNAT2 silencing with siRNA on amino acids in L6-G8C5 myoblasts. SNAT2 protein expression in this experiment is shown in Figure 4C. (A) SNAT2 transporter activity assessed from the rate of uptake of ^{14}C-MeAIB. (B) Intracellular L-Gln concentration. (C) Intracellular L-Leu concentration. (Data for other amino acids are presented in Table 2.) Twenty-four hours after removal of transfection agent, cultures were incubated for an additional 3 h in minimum essential medium (MEM; pH 7.4) with 2% dialyzed serum before preparation of amino acid extracts. *$P <$ 0.05 *versus* Scr. Results from one experiment representative of three independent experiments are shown (n = 3 to 4 replicate culture wells for each treatment).

Table 2. Effect of SNAT2 silencing with siRNA on intracellular free amino acid profile in L6-G8C5 myoblasts[a]

Amino Acid	Concentration in Fresh MEM (μmol/L)	Intracellular Free Amino Acid Concentration (nmol/mg protein)		
		Transfection Blank	Scrambled siRNA	Silencing siRNA
L-Ala	Nil	50.8 ± 7.7	38.9 ± 1.0	61.8 ± 3.3[c]
L-Arg	600	6.5 ± 1.0	5.7 ± 0.2	5.7 ± 0.3
L-Asn	Nil	1.01 ± 0.11	0.99 ± 0.03	0.96 ± 0.04
L-Asp	Nil	16.6 ± 2.2	14.0 ± 0.7	16.5 ± 0.6
L-Cys	200[b]	UD	UD	UD
L-Glu	Nil	94.4 ± 13.2	88.9 ± 3.8	80.3 ± 3.9
Gly	Nil	7.4 ± 1.3	3.9 ± 0.8[d]	3.2 ± 0.3[d]
L-His	200	5.6 ± 0.7	4.2 ± 0.9	1.9 ± 0.1[c,d]
L-Ile	400	5.7 ± 0.4	5.4 ± 0.3	3.9 ± 0.2[c]
L-Lys	400	3.7 ± 0.1	3.8 ± 0.2	3.9 ± 0.2
L-Met	100	2.6 ± 0.4	2.9 ± 0.1	1.6 ± 0.1[c]
L-Phe	200	4.3 ± 0.6	4.1 ± 0.2	3.1 ± 0.1[c]
L-Pro	Nil	4.2 ± 0.1	4.2 ± 0.5	4.8 ± 0.4
L-Ser	Nil	1.26 ± 0.15	1.27 ± 0.04	1.31 ± 0.16
L-Thr	400	29.0 ± 3.0	25.7 ± 1.0	19.8 ± 0.9[c]
L-Trp	50	1.39 ± 0.21	1.34 ± 0.06	1.00 ± 0.05[c]
L-Tyr	200	4.6 ± 0.7	4.4 ± 0.2	3.2 ± 0.2[c]
L-Val	400	5.6 ± 0.9	5.2 ± 0.2	4.0 ± 0.2[c]

[a]Data for L-Gln and L-Leu are presented in Figure 5. Results from one experiment representative of three independent experiments are shown ($n = 4$ replicate culture wells for each treatment). Silencing of SNAT2 protein expression in this experiment is shown in Figure 4C. siRNA, small interfering RNA.
[b]Added as cystine.
[c]$P < 0.05$ *versus* scrambled siRNA.
[d]$P < 0.05$ *versus* transfection blank.

SNAT2 Is a Potential Regulator of mTOR Signaling to Protein Synthesis

Stimulation of protein phosphorylation events downstream of mTOR has been demonstrated previously in L6 myotubes in response to L-Leu (33) and may respond to other amino acids. Depletion of amino acids by SNAT2 inhibition would therefore be predicted to blunt such phosphorylation signals. For phosphorylation of rpS6, this was clearly demonstrated when SNAT2 was inhibited with MeAIB or by low pH in L6 myotubes that had been stimulated with 2% serum or 100 nM insulin (Figures 6A and 7B). A similar result was obtained for S6 kinase activation detected by mobility shift (Figure 6B) and for 4E-BP1 phosphorylation (Figure 6C).

To test the possibility that MeAIB exerts its effects in Figure 6 by acutely blocking amino acid sensing by the cells, rather than through its actions on SNAT2, we also performed experiments in cultures that were preincubated for 4 h with MeAIB, followed by thorough rinsing and incubation with medium without MeAIB. SNAT2 is known to upregulate when starved of its amino acid substrates (28) and, conversely, downregulates when substrate loaded. After 4 h of preincubation with 10 mM MeAIB, SNAT2 transporter activity was strongly downregulated (Figure 7A), and detectable downregulation persisted for a further 2h in medium without MeAIB (Figure 7A). Such preincubation also led to impairment of rpS6 phosphorylation (Figure 7B), suggesting that MeAIB acts *via* SNAT2 rather than through acute effects on amino acid sensing. Impairment of rpS6 phosphorylation by SNAT2 inhibition was also confirmed by silencing SNAT2 with siRNA (Figure 6D).

Functional Effects of SNAT2 on Protein Metabolism

Effects of pH and MeAIB. In myotubes, the effect of low pH on mTOR signaling in Figures 6 and 7 was accompanied by a sustained 48-h impairment of global protein synthesis (Figure 8C) and a decrease in total protein (10 ± 2% decrease in 48-h *versus* pH 7.4 cultures; $P < 0.05$). Similarly, in myoblasts, 24 h of incubation at pH 7.1 decreased total protein content and impaired protein synthesis (Table 3). The acidosis effect on protein synthesis in myotubes was blunted by 10 nM rapamycin, a dosage that almost abolishes signaling to rpS6 (Figure 8, A and C), suggesting that signaling through mTOR is involved. The effect was also blunted by extracellular L-Gln deprivation (Figure 8C), suggesting that it is mediated at least partly by effects on L-Gln.

We showed previously in L6 myotubes that antagonism of amino acid influx through SNAT2 with as little as 1 mM MeAIB in the presence of 2 mM L-Gln stimulates protein degradation within 7 h (18), an effect that is blunted by extracellular L-Gln deprivation or L-Gln loading, suggesting that MeAIB acts at least partly by antagonizing L-Gln influx (18). In this study with myotubes in the presence of 2 mM L-Gln, MeAIB also significantly impaired global protein synthesis within 2 h at dosages down to 1 mM (Figure 8B). This impairment was sustained for at least 48 h (Figure 8D), was comparable in magnitude with the impairment that was seen with rapamycin or L-Gln starvation (Figure 8, C and D), and was accompanied by a decline in total protein (16 ± 2% decrease in 48 h; $P < 0.05$). The magnitude of this inhibition of protein synthesis was blunted by extracellular L-Gln deprivation (30 ± 4% decrease; $P < 0.05$; Figure 8D) and

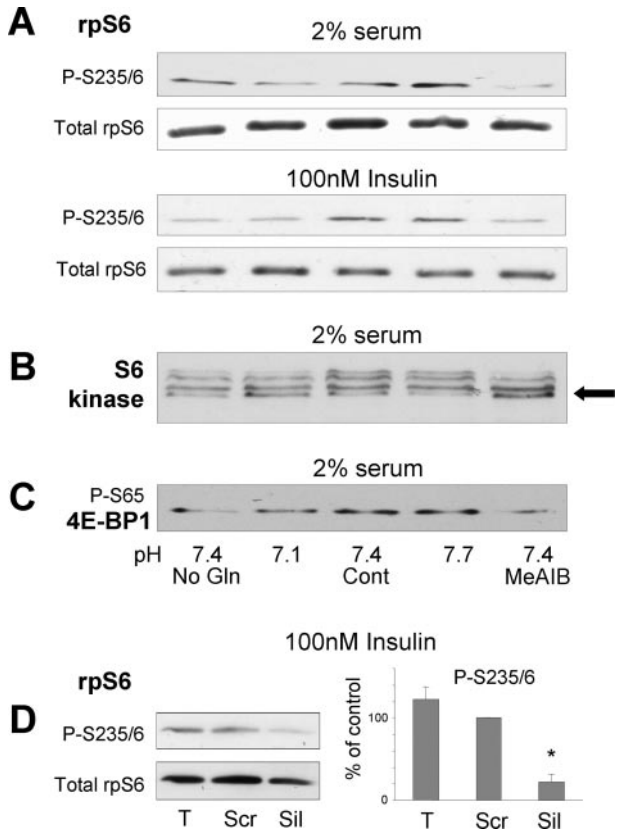

Figure 6. (A through C) Effect of 2 h of extracellular L-Gln starvation, pH variation, or inhibition of SNAT2 transporters with 10 mM MeAIB on mammalian target of rapamycin (mTOR)-dependent signaling in L6-G8C5 myotubes that were incubated in MEM with 2% dialyzed serum or serum-free medium with 100 nM bovine insulin. Proteins were separated by SDS-PAGE and immunoblotted using specific antibodies. Blots representative of at least three independent experiments are presented as follows: (A) Ribosomal protein S6 (rpS6) phosphorylated at Ser residue 235/6. Quantification of rpS6 phosphorylation by densitometry is presented in Figure 7. (B) Ribosomal protein S6 kinase (irrespective of its state of phosphorylation). Mobility shifting of the main bands in MeAIB-treated cultures (black arrow) relative to the pH 7.4 control cultures indicates impaired phosphorylation/activation of rpS6 kinase. (C) Eukaryotic initiation factor 4E binding protein 1 (4E-BP1) phosphorylated at Ser residue 65. In four independent experiments, the phosphorylation signal with MeAIB (quantified by densitometry) was 53 ± 9% of the pH 7.4 Control value, $P < 0.05$. (D) Effect of SNAT2 silencing with siRNA on rpS6 phosphorylation. Twenty-four hours after removal of transfection agent, cultures were incubated for an additional 2 h in serum-free MEM (pH 7.4) with 100 nM bovine insulin. The bar graph denotes quantification of phosphorylation by densitometry from five independent experiments expressed as percentage of the Scr control value. *$P < 0.05$ *versus* Scr.

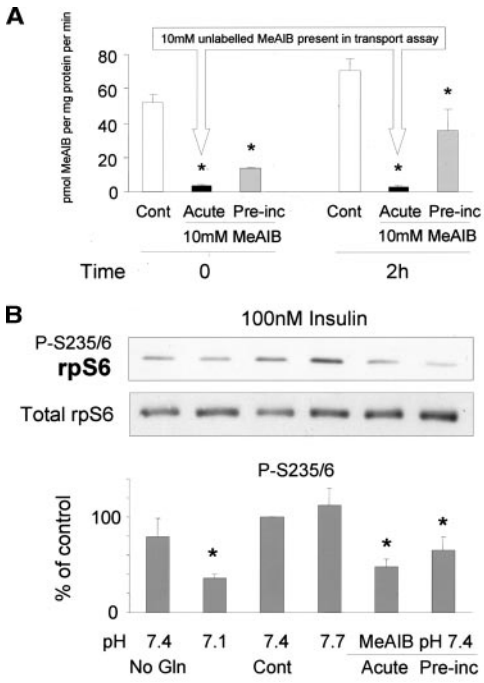

Figure 7. (A) Effect on SNAT2 transporter activity of acute incubation (Acute) or prolonged preincubation (Preinc) with MeAIB. L6-G8C5 myotubes were incubated for 4 h in MEM/2% FBS with (Preinc) or without (Cont and Acute) 10 mM MeAIB. Time 0 cultures were then rinsed three times with HBSS, and SNAT2 transporter activity (uptake of ^{14}C-MeAIB calculated using a specific radioactivity of 50 mCi [1.85 GBq]/mmol) was immediately measured (see Materials and Methods). Time 2-h cultures received an additional 2 h of incubation in serum-free MEM at pH 7.4 with 100 nM bovine insulin with (Acute) or without (Cont and Preinc) 10 mM MeAIB. Uptake of ^{14}C-MeAIB was then measured immediately at the end of the 2-h incubation. In Acute cultures, 10 mM MeAIB was present throughout the 2-h incubation and during both the time 0 and 2 h ^{14}C-MeAIB uptake assays: ^{14}C-MeAIB uptake in these cultures reflects nonspecific binding rather than transport into the cells. *$P < 0.05$ *versus* the corresponding Cont cultures. Results from one experiment representative of three independent experiments are shown ($n = 3$ replicate culture wells for each treatment). (B) Effect on rpS6 phosphorylation of Acute or Preinc with MeAIB. Cultures were incubated as in the experiment with bovine insulin in Figure 6A, but those with MeAIB were either incubated acutely (Acute) for 2 h or preincubated (Preinc) for 4 h followed by removal of MeAIB for the last 2 h, exactly as described in A. Immunoblotting was performed as in Figure 6A. The bar graph denotes quantification of rpS6 phosphorylation by densitometry from 15 independent experiments (six for Preinc) expressed as percentage of the pH 7.4 Control value. *$P < 0.05$ *versus* Cont.

abolished in medium loaded with 22 mM L-Gln (Figure 8D), again suggesting that antagonism of L-Gln by MeAIB was a contributor. In myoblasts, complete inhibition of SNAT2 with 10 mM MeAIB impaired protein synthesis, stimulated protein degradation, and decreased total protein without loss of cell viability (Table 3). However, unlike myotubes (18), partial inhibition of SNAT2 with low pH had no effect on protein degradation (Table 3), and partial competitive inhibition of SNAT2 with lower dosages of MeAIB (0.5 to 2 mM) gave negligible stimulation of protein degradation (data not shown), suggest-

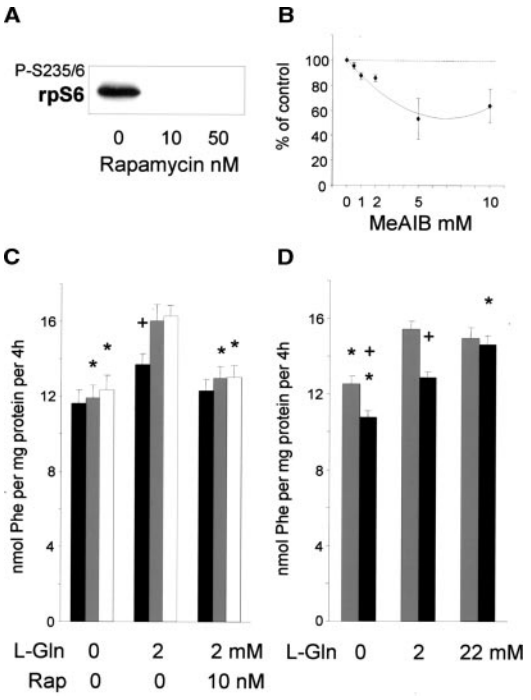

Figure 8. (A) Inhibition of mTOR signaling with rapamycin in L6-G8C5 myotubes. Phosphorylation of rpS6 after 2 h in MEM (pH 7.4) with 2% dialyzed serum and the specified dosage of rapamycin was detected exactly as described in Figure 6A. Identical results were obtained with 100 nM bovine insulin in place of serum. (B through D) Effects of pH or SNAT2 inhibition on protein synthesis rate (^{3}H-L-Phe incorporation) in L6-G8C5 myotubes. Pooled data from three independent experiments ($n = 3$ replicate culture wells for each treatment). (B) Dosage-response curve for acute inhibition of protein synthesis by MeAIB. Myotubes were incubated for 2 h in MEM (pH 7.4) with 2% dialyzed serum and the specified dosage of MeAIB. ^{3}H-L-Phe was present in the medium for the final 30 min of the incubation. Synthesis rate is expressed as percentage of the rate in control cultures without MeAIB. Significant ($P < 0.05$) inhibition was observed at all dosages >0.5 mM. (C) Effect of prolonged acidosis on protein synthesis rate. Myotubes were incubated for 48 h in MEM with 2% dialyzed serum and the specified concentrations of L-Gln or rapamycin at pH 7.1 (■), pH 7.4 (▨), or pH 7.7 (□). $^*P < 0.05$ *versus* the corresponding value at the same pH with 2 mM L-Gln and without rapamycin; $^+P < 0.05$ *versus* the corresponding value at pH 7.4. (D) Effect of prolonged SNAT2 inhibition with MeAIB on protein synthesis rate. Myotubes were incubated for 48 h in MEM (pH 7.4) with 2% dialyzed serum and the specified concentrations of L-Gln in medium with 10 mM MeAIB (■) or no MeAIB (▨). $^*P < 0.05$ *versus* the corresponding value with 2 mM L-Gln; $^+P < 0.05$ *versus* the value at the same L-Gln concentration without MeAIB.

ing that protein degradation in myoblasts is less responsive to SNAT2 than in myotubes.

Effects of SNAT2 Silencing. The functional importance of SNAT2 in protein metabolism was confirmed by silencing SNAT2 in L6 myoblasts with siRNA (Table 4). SNAT2 silencing significantly decreased the protein content of the cultures (Table 4). This was not attributable to cell toxicity (protein leakage or cell detachment) because protein release into the medium decreased rather than increased when SNAT2 was silenced (Table 4). In agreement with the lack of effect of low pH on protein degradation in myoblasts (Table 3), the partial silencing of SNAT2 activity (76% inhibition) had no stimulatory effect on protein degradation (Table 4). However, the protein synthesis rate was lower in the silenced cultures (Table 4), commensurate with the decline in synthesis that was observed with low pH or MeAIB in Table 3.

Discussion

SNAT2 Determines L-Gln Concentration in L6-G8C5 Cells

This study is the first demonstration that selective inhibition of a single transporter protein, SNAT2 (slc38 A2), leads to marked depletion of L-Gln in cultured skeletal muscle cells. At first glance, this is surprising because a wide range of amino acid transporter genes are expressed in muscle and a number of these transport L-Gln (36). Not all of these, however, directly accumulate L-Gln inside cells against its concentration gradient. For example, ASC transporters (slc1 A4 and A5) and System L transporters (slc7 A5 and A8) are primarily amino acid exchangers (36) and consequently have only secondary effects on intracellular L-Gln concentration. Transporters of the SNAT/slc38 family other than SNAT2 can transport L-Gln against a gradient (19) but are unlikely to contribute to L-Gln accumulation in L6 cells because they are expressed only at low level (Figure 4A). A similar situation applies in muscle *in vivo*, where the predominant SNAT transporter expressed is again SNAT2 (27,28). Of the other System A transporters, SNAT1 is expressed only at low level (19), and SNAT4 is unlikely to be a major contributor because L-Gln is only a weak substrate for this transporter (37). The low levels of N-type transporters SNAT3 and SNAT5 in muscle are also unlikely to drive intracellular L-Gln accumulation in view of their role in L-Gln efflux (38).

Inhibition of SNAT2 Depletes Amino Acids That Are Not Transported on SNAT2

It is important to note that selective inhibition of SNAT2 led to depletion of other amino acids that are not regarded as SNAT2 substrates (Figures 1B and 5C, Tables 1 and 2), suggesting that SNAT2 also exerts indirect effects. This is consistent with reports that System A transporters, particularly SNAT2 (39) "energize" the active accumulation of amino acids through other transporters, notably System L, by building a transmembrane L-Gln gradient that then drives active uptake of other amino acids, such as L-Leu, by exchange of intracellular L-Gln for extracellular L-Leu (Figure 1D). Manipulation of the transmembrane L-Gln and L-Leu gradients in L6-G8C5 myotubes followed by measurement of changes in intracellular L-Leu and L-Gln, respectively, confirmed the presence of such effects in this study (Figures 1 through 3). This suggests that SNAT2 is an important determinant of the intracellular concentration of amino acids that are thought to exert a protein anabolic effect in muscle (L-Gln, L-Leu, L-Ile, and L-Val).

Table 3. Functional effects on global protein metabolism of inhibiting SNAT2 for 24 h with low pH or MeAIB in L6-G8C5 myoblasts[a]

Parameter	Composition of the Experimental Medium (pH)			
	7.1	7.4 (Control)	7.7	7.4
L-Gln (mmol/L)	2	2	2	2
MeAIB (mmol/L)	0	0	0	10
Total protein t = 28 h				
μg/35-mm well	174 ± 17	212 ± 11	195 ± 15	165 ± 18[b]
% of pH 7.4 control value	81 ± 6[b]	100	92 ± 5	77 ± 7[b]
Protein synthesis rate t = 24 to 28 h				
nmol L-Phe/mg protein in 4 h	8.8 ± 0.3[c]	9.9 ± 0.5	10.3 ± 0.3	8.15 ± 0.12[b]
% of pH 7.4 control value	89 ± 3[b]	100	104 ± 3	82 ± 1[b]
Protein degradation rate t = 26 to 33 h				
$\log_{10}$%/h × 10^3	10.8 ± 0.9	10.5 ± 0.9	10.4 ± 1.1	13.6 ± 1.0
% of pH 7.4 control value	102 ± 2	100	98 ± 2	130 ± 2[b]
Intact protein leakage (cell damage indicator) t = 26 to 33 h				
% per h	0.13 ± 0.01	0.16 ± 0.01	0.17 ± 0.02	0.15 ± 0.02
% of pH 7.4 control value	80 ± 8	100	102 ± 8	94 ± 8

[a]Pooled data from three experiments are shown (with three replicate culture wells for each treatment). Cells were incubated in the experimental medium (MEM + 2% dialyzed FBS with the additions stated) for 24 h. All measurements were then made in parallel at the times (t) indicated using fresh samples of the same experimental medium.
[b]$P < 0.05$ *versus* pH 7.4 control.
[c]$P < 0.05$ *versus* pH 7.7.

Table 4. Functional effects on global protein metabolism of 24 h of SNAT2 silencing with siRNA in L6-G8C5 myoblasts[a]

	Transfection Blank	Control Scrambled siRNA	Silencing siRNA
SNAT2 Transporter Activity t = 24 h			
pmol MeAIB/mg protein per min	227 ± 48	249 ± 56	63 ± 19[b]
% of control value	97 ± 10	100	24 ± 7[b]
Total protein t = 28 h			
μg/35-mm well	316 ± 55	284 ± 40	203 ± 31
% of control value	106 ± 15	100	71 ± 5[b]
Protein synthesis rate t = 24 to 28 h			
nmol L-Phe/mg protein in 4 h	9.1 ± 1.2	9.2 ± 1.2	8.2 ± 1.1
% of control value	99 ± 1	100	88 ± 2[b]
Protein degradation rate t = 26 to 33 h			
$\log_{10}$%/h × 10^3	7.3 ± 0.4	7.7 ± 0.4	7.4 ± 0.4
% of control value	94 ± 6	100	97 ± 5
Intact protein leakage (cell damage indicator) t = 26 to 33 h			
% per h	0.11 ± 0.02	0.14 ± 0.03	0.09 ± 0.01
% of control value	84 ± 6[b]	100	73 ± 6[b]

[a]Pooled data from three experiments are shown (with three replicate culture wells for each treatment). Cells were transfected with SNAT2 silencing siRNA or scrambled control siRNA as described in Materials and Methods. Transfection was followed by a 24-h incubation in DMEM + 10% FBS. All measurements were then made in parallel at the times indicated in MEM at pH 7.4 with 2% dialyzed FBS. The times (t) denote the time elapsed since removal of the transfection agent.
[b]$P < 0.05$ *versus* scrambled control siRNA.

SNAT2 Regulates mTOR and Influences Protein Metabolism

Signaling effects through amino acid transporters are now a well-established concept in mammalian cell biology (36). Although much remains to be learned about signaling pathways that are affected by SNAT2, the data in Figures 6 and 7 suggest that the level of SNAT2 inhibition by acidosis exerts functionally significant effects on mTOR, consistent with an earlier report of co-regulation of SNAT2 and mTOR in L6 cells that were treated with ceramide (17). Acute inhibition of the flux through SNAT2 by treating with MeAIB could in principle exert nonspecific effects (independent of SNAT2) because MeAIB is itself an amino acid analogue and might influence amino acid sensing by the cell. This

is unlikely to be the explanation, however, because preincubation with MeAIB, which downregulates SNAT2 transport, followed by a 2-h washout period without MeAIB, also led to impaired rpS6 phosphorylation (Figure 7B), suggesting that MeAIB is more likely to be acting on SNAT2. A similar impairment of rpS6 signaling was obtained by silencing SNAT2 with siRNA (Figure 6D), and these effects on mTOR were followed by sustained effects on protein metabolism (Figure 8, Tables 3 and 4). These observations are functionally important because System A/SNAT2 transporters upregulate in muscle in response to exercise (40) (and presumably downregulate in sedentary renal patients), and mTOR signaling is a key link between mechanical loading of muscle and the resulting stimulation of protein synthesis (41,42). It is still unclear, however, which amino acids that are affected by SNAT2 mediate the effects of SNAT2 on mTOR and protein metabolism.

SNAT2 Inhibition Mimics the Effects of Acidosis In Vivo

A recent site-directed mutagenesis study showed that SNAT2 inhibition by low pH is largely a consequence of protonation of the extracellular carboxyterminal histidine residue (20). The fall in interstitial fluid pH that occurs even during compensated metabolic acidosis *in vivo* (43,44) would therefore be expected to inhibit SNAT2 directly. Inhibition of System A/SNAT2 activity has been reported *in vivo* in skeletal muscle of patients with chronic renal failure (45), and persistent inhibition has been demonstrated during *ex vivo* incubation of muscles from uremic rats (46), suggesting that uremic factors other than protonation also inhibit SNAT2. The pattern of amino acid depletion that was observed in this study resembles the changes in intramuscular amino acid concentrations and muscle/plasma concentration gradients that were reported in hemodialysis patients (5,6). The mechanisms reported here may therefore be relevant to the initiation of amino acid depletion and impaired protein metabolism *in vivo*. Finally, these effects may be particularly important in renal patients with diabetes. In view of their preexisting insulin deficiency or insulin resistance, the inhibition of amino acid–dependent insulin signaling through mTOR after SNAT2 inhibition may explain why muscle protein metabolism is so badly impaired in these patients (1). It will now be interesting to determine whether other pathways of insulin signaling in addition to mTOR are impaired by inhibiting SNAT2.

Acknowledgments

We gratefully acknowledge grants from Kidney Research UK (RP26/2/2004), Wellcome Trust (059828/Z/99/Z), Jules Thorn Trust (03SC/06A), Peel Medical Research Trust (AGT.R5), and Renal Care and Research Association. K.F.E. thanks Kidney Research UK and Diabetes UK for studentship DUK ST3/2004.

Disclosures

None.

References

1. Pupim LB, Heimburger O, Qureshi AR, Ikizler TA, Stenvinkel P: Accelerated lean body mass loss in incident chronic dialysis patients with diabetes mellitus. *Kidney Int* 68: 2368–2374, 2005
2. Mitch WE: Metabolic and clinical consequences of metabolic acidosis. *J Nephrol* 19[Suppl 9]: S70–S75, 2006
3. Stein A, Moorhouse J, Iles-Smith H, Baker F, Johnstone J, James G, Troughton J, Bircher G, Walls J: Role of an improvement in acid-base status and nutrition in CAPD patients. *Kidney Int* 52: 1089–1095, 1997
4. Szeto CC, Wong TY, Chow KM, Leung CB, Li PK: Oral sodium bicarbonate for the treatment of metabolic acidosis in peritoneal dialysis patients: A randomized placebo-control trial. *J Am Soc Nephrol* 14: 2119–2126, 2003
5. Bergstrom J, Alvestrand A, Furst P: Plasma and muscle free amino acids in maintenance hemodialysis patients without protein malnutrition. *Kidney Int* 38: 108–114, 1990
6. Lofberg E, Wernerman J, Anderstam B, Bergstrom J: Correction of acidosis in dialysis patients increases branched-chain and total essential amino acid levels in muscle. *Clin Nephrol* 48: 230–237, 1997
7. Proud CG: mTOR-mediated regulation of translation factors by amino acids. *Biochem Biophys Res Commun* 313: 429–436, 2004
8. Kleger GR, Turgay M, Imoberdorf R, McNurlan MA, Garlick PJ, Ballmer PE: Acute metabolic acidosis decreases muscle protein synthesis but not albumin synthesis in humans. *Am J Kidney Dis* 38: 1199–1207, 2001
9. Vabulas RM, Hartl FU: Protein synthesis upon acute nutrient restriction relies on proteasome function. *Science* 310: 1960–1963, 2005
10. Du J, Hu Z, Mitch WE: Molecular mechanisms activating muscle protein degradation in chronic kidney disease and other catabolic conditions. *Eur J Clin Invest* 35: 157–163, 2005
11. Curi R, Lagranha CJ, Doi SQ, Sellitti DF, Procopio J, Pithon-Curi TC, Corless M, Newsholme P: Molecular mechanisms of glutamine action. *J Cell Physiol* 204: 392–401, 2005
12. Holecek M: Relation between glutamine, branched-chain amino acids, and protein metabolism. *Nutrition* 18: 130–133, 2002
13. Lyons SD, Sant ME, Christopherson RI: Cytotoxic mechanisms of glutamine antagonists in mouse L1210 leukemia. *J Biol Chem* 265: 11377–11381, 1990
14. Oehler R, Roth E: Regulative capacity of glutamine. *Curr Opin Clin Nutr Metab Care* 6: 277–282, 2003
15. Rennie MJ, Hundal HS, Babij P, MacLennan P, Taylor PM, Watt PW, Jepson MM, Millward DJ: Characteristics of a glutamine carrier in skeletal muscle have important consequences for nitrogen loss in injury, infection, and chronic disease. *Lancet* 2: 1008–1012, 1986
16. Mittendorfer B, Volpi E, Wolfe RR: Whole body and skeletal muscle glutamine metabolism in healthy subjects. *Am J Physiol Endocrinol Metab* 280: E323–E333, 2001
17. Hyde R, Hajduch E, Powell DJ, Taylor PM, Hundal HS: Ceramide down-regulates system A amino acid transport and protein synthesis in rat skeletal muscle cells. *FASEB J* 19: 461–463, 2005
18. Bevington A, Brown J, Butler H, Govindji S, M-Khalid K, Sheridan K, Walls J: Impaired system A amino acid transport mimics the catabolic effects of acid in L6 cells. *Eur J Clin Invest* 32: 590–602, 2002
19. Mackenzie B, Erickson JD: Sodium-coupled neutral amino acid (system N/A) transporters of the SLC38 gene family. *Pflugers Arch* 447: 784–795, 2004

20. Baird FE, Pinilla-Tenas JJ, Ogilvie WL, Ganapathy V, Hundal HS, Taylor PM: Evidence for allosteric regulation of pH-sensitive system A (SNAT2) and system N (SNAT5) amino acid transporter activity involving a conserved histidine residue. *Biochem J* 397: 369–375, 2006
21. Gomez E, Powell ML, Greenman IC, Herbert TP: Glucose-stimulated protein synthesis in pancreatic beta-cells parallels an increase in the availability of the translational ternary complex (eIF2-GTP.Met-tRNAi) and the dephosphorylation of eIF2 alpha. *J Biol Chem* 279: 53937–53946, 2004
22. Hajduch E, Alessi DR, Hemmings BA, Hundal HS: Constitutive activation of protein kinase B alpha by membrane targeting promotes glucose and system A amino acid transport, protein synthesis, and inactivation of glycogen synthase kinase 3 in L6 muscle cells. *Diabetes* 47: 1006–1013, 1998
23. Bevington A, Brown J, Pratt A, Messer J, Walls J: Impaired glycolysis and protein catabolism induced by acid in L6 rat muscle cells. *Eur J Clin Invest* 28: 908–917, 1998
24. Ballard FJ, Francis GL: Effects of anabolic agents on protein breakdown in L6 myoblasts. *Biochem J* 210: 243–249, 1983
25. Hundal HS, Bilan PJ, Tsakiridis T, Marette A, Klip A: Structural disruption of the trans-Golgi network does not interfere with the acute stimulation of glucose and amino acid uptake by insulin-like growth factor I in muscle cells. *Biochem J* 297: 289–295, 1994
26. Khym JX: An analytical system for rapid separation of tissue nucleotides at low pressures on conventional anion exchangers. *Clin Chem* 21: 1245–1252, 1975
27. Yao D, Mackenzie B, Ming H, Varoqui H, Zhu H, Hediger MA, Erickson JD: A novel system A isoform mediating Na+/neutral amino acid cotransport. *J Biol Chem* 275: 22790–22797, 2000
28. Hyde R, Christie GR, Litherland GJ, Hajduch E, Taylor PM, Hundal HS: Subcellular localization and adaptive up-regulation of the system A (SAT2) amino acid transporter in skeletal-muscle cells and adipocytes. *Biochem J* 355: 563–568, 2001
29. Xiang J, Ennis SR, Abdelkarim GE, Fujisawa M, Kawai N, Keep RF: Glutamine transport at the blood-brain and blood-cerebrospinal fluid barriers. *Neurochem Int* 43: 279–288, 2003
30. Ensenat D, Hassan S, Reyna SV, Schafer AI, Durante W: Transforming growth factor-beta 1 stimulates vascular smooth muscle cell L-proline transport by inducing system A amino acid transporter 2 (SAT2) gene expression. *Biochem J* 360: 507–512, 2001
31. Al-Bader MD, Al-Sarraf HA: Housekeeping gene expression during fetal brain development in the rat-validation by semi-quantitative RT-PCR. *Brain Res Dev Brain Res* 156: 38–45, 2005
32. Lundholm K, Edstrom S, Ekman L, Karlberg I, Walker P, Schersten T: Protein degradation in human skeletal muscle tissue: The effect of insulin, leucine, amino acids and ions. *Clin Sci (Lond)* 60: 319–326, 1981
33. Kimball SR, Shantz LM, Horetsky RL, Jefferson LS: Leucine regulates translation of specific mRNAs in L6 myoblasts through mTOR-mediated changes in availability of eIF4E and phosphorylation of ribosomal protein S6. *J Biol Chem* 274: 11647–11652, 1999
34. Bevington A, Brown J, Walls J: Leucine suppresses acid-induced protein wasting in L6 rat muscle cells. *Eur J Clin Invest* 31: 497–503, 2001
35. Christensen HN, Oxender DL, Liang M, Vatz KA: The use of N-methylation to direct route of mediated transport of amino acids. *J Biol Chem* 240: 3609–3616, 1965
36. Hyde R, Taylor PM, Hundal HS: Amino acid transporters: Roles in amino acid sensing and signalling in animal cells. *Biochem J* 373: 1–18, 2003
37. Sugawara M, Nakanishi T, Fei YJ, Martindale RG, Ganapathy ME, Leibach FH, Ganapathy V: Structure and function of ATA3, a new subtype of amino acid transport system A, primarily expressed in the liver and skeletal muscle. *Biochim Biophys Acta* 1509: 7–13, 2000
38. Baird FE, Beattie KJ, Hyde AR, Ganapathy V, Rennie MJ, Taylor PM: Bidirectional substrate fluxes through the system N (SNAT5) glutamine transporter may determine net glutamine flux in rat liver. *J Physiol* 559: 367–381, 2004
39. Franchi-Gazzola R, Dall'asta V, Sala R, Visigalli R, Bevilacqua E, Gaccioli F, Gazzola GC, Bussolati O: The role of the neutral amino acid transporter SNAT2 in cell volume regulation. *Acta Physiol (Oxf)* 187: 273–283, 2006
40. King PA: Effects of insulin and exercise on amino acid transport in rat skeletal muscle. *Am J Physiol* 266: C524–C530, 1994
41. Cuthbertson DJ, Babraj J, Smith K, Wilkes E, Fedele MJ, Esser K, Rennie M: Anabolic signaling and protein synthesis in human skeletal muscle after dynamic shortening or lengthening exercise. *Am J Physiol Endocrinol Metab* 290: E731–E738, 2006
42. Hornberger TA, Stuppard R, Conley KE, Fedele MJ, Fiorotto ML, Chin ER, Esser KA: Mechanical stimuli regulate rapamycin-sensitive signalling by a phosphoinositide 3-kinase-, protein kinase B- and growth factor-independent mechanism. *Biochem J* 380: 795–804, 2004
43. Steinhagen C, Hirche HJ, Nestle HW, Bovenkamp U, Hosselmann I: The interstitial pH of the working gastrocnemius muscle of the dog. *Pflugers Arch* 367: 151–156, 1976
44. Wesson DE: Dietary acid increases blood and renal cortical acid content in rats. *Am J Physiol* 274: F97–F103, 1998
45. Asola MR, Virtanen KA, Peltoniemi P, Nagren K, Jyrkkio S, Knutti J, Nuutila PR, Metsarinne KP: Amino acid transport into skeletal muscle is impaired in chronic renal failure [Abstract]. *J Am Soc Nephrol* 12: 64A, 2001
46. Maroni BJ, Haesemeyer RW, Kutner MH, Mitch WE: Kinetics of system A amino acid uptake by muscle: Effects of insulin and acute uremia. *Am J Physiol* 258: F1304–F1310, 1990